

AN ABSTRACT OF THE THESIS OF

SATYA PAL KHANNA for the M. S. in ELECTRICAL ENGINEERING  
(Name) (Degree) (Major)

Date thesis is presented 8-5-63

Title THE CONCENTRATION PROFILE OF DIFFUSED  
RADIO-ACTIVE ANTIMONY IN A SILICON-DIOXIDE LAYER

Abstract approved   
(Major professor)

The selective masking effect of a thermally grown layer of silicon dioxide has been widely utilized as a technique for controlling the geometry and impurity concentration in semi-conductor device technology. It is also recognized that the passivation of the silicon surface by the vitreous silicon dioxide envelope protects the underlying surface from damage during the diffusion process. Thus indirectly it helps in improving the device parameters, like current amplification factor, the reverse current and the breakdown voltage.

In spite of its very wide application in device design the physics of the effect is hardly understood. Very little work has been done in this field. The mechanism of the chemical reduction of the impurity oxide in the silicon dioxide layer and its distribution therein should have a strong influence on the concentration of the impurity in silicon. The present endeavor was concerned with finding the distribution of

antimony, one of the donor elements, in the oxide layer.

The experimental evidence indicates that the migration of antimony through silicon dioxide is a diffusion controlled reaction and that its concentration profile can be broken up into two regions. The diffusion follows an approximate erfc distribution in the first region with diffusion constant =  $7.40 \times 10^{-15} \text{ cm}^2/\text{sec}$ . The second region, however, shows a saturation behavior.

THE CONCENTRATION PROFILE OF DIFFUSED  
RADIO-ACTIVE ANTIMONY IN A SILICON-DIOXIDE LAYER

by

SATYA PAL KHANNA

A THESIS

submitted to

OREGON STATE UNIVERSITY

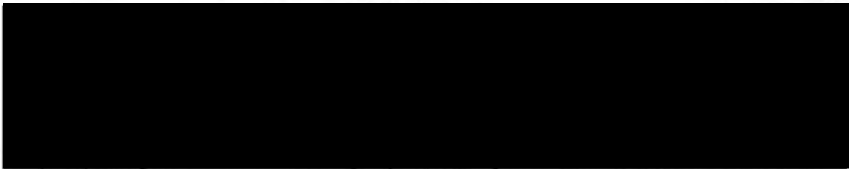
in partial fulfillment of  
the requirements for the  
degree of

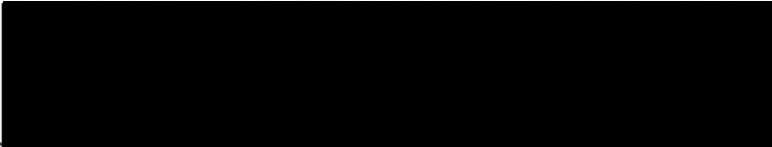
MASTER OF SCIENCE

August 1963

APPROVED:

  
Assistant Professor of Electrical Engineering  
In Charge of Major

  
Head of Department of Electrical Engineering

  
Dean of Graduate School

Date thesis is presented 8-5-63

Typed by Jolene Hunter Wuest

## ACKNOWLEDGMENT

The author wishes to thank Professor James C. Looney of Electrical Engineering Department, Oregon State University for his constructive suggestions and help during this research. Thanks are also due to Professor Olaf G. Paasche of Mechanical Engineering Department for permission to use metallographic microscope and to Dr. Chih H. Wang for making available the facilities of the Radiation Research Department. It is also a pleasure to acknowledge the assistance of Mr. Stevens P. Tucker in the preparation of the photographic plates and of my wife in the analysis of the data and typing.

## TABLE OF CONTENTS

	<u>Page</u>
INTRODUCTION	1
DIFFUSION	4
Diffusion Mechanism	4
The Diffusion Coefficient	6
Boundary Value Problems in Diffusion	7
Diffusion Methods	12
Measurements of Diffusion in Silicon	13
Diffusion Into Silicon Through an Oxide Layer	17
DIFFUSION OF ANTIMONY THROUGH A SILICON DIOXIDE LAYER	21
Sample Preparation	22
Growing Oxide Layers and Measurement of Their Thickness	23
Layer Sectioning	28
Diffusion Process	31
Detection of Impurity Distribution	32
Final Experiment	35
EXPERIMENTAL RESULTS AND DISCUSSION	38
BIBLIOGRAPHY	44
APPENDIX	47

## LIST OF FIGURES AND PLATES

Figure		Page
1	Step-function solution of the diffusion equation	9
2	Origin of wedge fringes	25
3	Oxide film step formation	25
4	Silicon dioxide film thickness	27
5	Etching rate	29
6	Diffusion furnace	33
7	Radio-active counts vs. oxide layer section	41
8	Comparison with erfc distribution	42
Plate		
I	Typical interference fringe photographs used to determine etching rates.	30
II	Interference fringe photographs of two samples used to determine final oxide layer thickness	34

# THE CONCENTRATION PROFILE OF DIFFUSED RADIO-ACTIVE ANTIMONY IN A SILICON-DIOXIDE LAYER

## INTRODUCTION

Semiconductor devices made from single crystals usually require the formation of p- and n-type regions within that crystal. Two common techniques to get these are alloying and diffusion. In alloying it is difficult to control the depth, and the impurity concentrations are limited to a narrow range of values. Diffusion as contrasted with alloying is a relatively slow process of introducing impurities into a semiconductor so that better depth and concentration controls are obtained. Solid state diffusion of impurities can be carried out by a variety of methods (5, 7, 8). Most published reports in this field follow the techniques initially described by Frosch and Derick (7). They carried out vapor-solid diffusion of donors and acceptors into silicon at atmospheric pressure. Their process consisted of heating the silicon wafers to approximately 1200°C and passing over them vapors from the heated impurity element with the help of a carrier gas. They found that gases such as helium or nitrogen cause serious pitting or erosion of the silicon surfaces. They also observed that if the silicon surface is covered by a thin vitreous silicon dioxide envelope, the underlying surface is completely protected against damage during the diffusion process. The desirability of surface passivation can be

appreciated in view of the effect of surface recombination on semiconductor device parameters. In the usual junction type transistor the current amplification factor is largely controlled by the properties of surface around the emitter; the reverse current at the collector may be greatly influenced by the surface nearby. The breakdown voltage too depends on the height of surface barriers near the collector.

In addition to surface protection, a silicon dioxide surface layer also provides a selective mask against the diffusion into silicon of some donor and acceptor impurity elements at high temperatures. The effect of masking in general depends on various conditions, namely, kind of impurity element and its vapor pressure, diffusion temperature and time etc., and it is necessary to study the degree of the masking effect as well as to make its mechanism clear.

The first attempt in this direction was made by Sah, Sello and Tremere (22) who studied the diffusion characteristics of phosphorus in silicon dioxide films. Using different thicknesses of silicon dioxide layers for phosphorus diffusion they inferred that an oxide of phosphorus diffuses through an apparently glassy layer of composition  $(P_x Si_y O_z)$  and upon reaching the interface between the glass and silicon dioxide it reacts with the latter to form a new

layer of glass. Thus the glass-silicon-dioxide interface advances with a velocity dependent on the diffusion rate of oxide of phosphorus in 'glass'. According to their conclusion the growth of glass follows a parabolic law. When the glass reaches the silicon-dioxide-silicon interface some phosphorus atoms enter silicon and diffuse away forming an n-p junction beneath the silicon surface.

Horiuchi and Yamaguchi (13) working on the diffusion of boron into silicon through an oxide layer also found a formation of a 'glassy' layer of unknown composition.

The purpose of the present endeavor is to study the diffusion of an oxide of antimony through a  $\text{SiO}_2$  layer and using radio-tracer techniques to find the concentration profile of antimony in different layers of a silicon dioxide envelope on a silicon wafer.

## DIFFUSION

### Diffusion Mechanism

From the theory of specific heats it is well known that atoms in a crystal oscillate about their equilibrium position. These oscillations will become violent if the atom acquires higher-than-normal energy. The atom might then jump from its own site to the neighboring one in the crystalline structure. Such interstitial transfer gives rise to diffusion in solids. If the high energy atom jumps to an unoccupied site the diffusion is said to be by a vacancy mechanism.

The diffusion of Group III and Group V elements in germanium and silicon is by a substitutional process [(11, p. 244) and (12, p. 165)]. Silicon crystallizes in a diamond lattice. If a silicon atom is replaced by an atom of an element from Group V, such as arsenic, there are five valence electrons from the arsenic to be disposed of. Four of these are shared with the four adjacent silicon atoms to form covalent bonds similar to those existing between contiguous silicon atoms. The fifth electron will not be held in any chemical bond but will be weakly attracted by arsenic by Coulomb force. However, its removal to a large distance leaves the arsenic with a net positive charge. The term donor derives from the fact

that the arsenic can 'donate' a conduction electron to the lattice.

In the replacement of a silicon atom by an element of Group III, indium for example, the three electrons contributed by the indium form covalent bonds with three of the four adjacent silicon atoms, but the fourth bond remains a one-electron bond i. e. a hole is formed. Just as the electron was weakly held to the arsenic by Coulomb forces, the hole is attracted to the indium. If it moves away, the fourth covalent bond to indium is completed, and the indium is left with a net negative charge. Group III elements are examples of acceptors, so-called because they can 'accept' electrons, thereby introducing holes into the valence band.

In Ge donors are found to diffuse more rapidly than the acceptors. This result can be explained on the basis of a smaller ionic radius of the donors or by means of a vacancy-impurity interaction model. Another suggestion is that since Ge vacancies behave as acceptors, they should show a higher probability of association with donor than with acceptor diffusants. This explanation assumes that diffusion is by a vacancy mechanism. Since silicon and germanium are such closely related elements one would expect similar results for diffusion in silicon. But silicon shows opposite behavior i. e. acceptors diffuse more rapidly than do the donors. The failure of this simple correlation in similar structures makes it

apparent that other interactions too come into play. These include the flow of atoms and ions, electrons and hole, heat, and defects such as vacancies; and forces made up of the gradients of electric potential, temperature and chemical potentials of all the components. Much of the work that has been done on diffusion in silicon and germanium has been aimed at obtaining values of diffusion constant  $D$  for the impurities of interest rather than on explaining the diffusion mechanism.

### The Diffusion Coefficient

The diffusion process can be mathematically expressed with the help of Fick's laws which are very general and do not take into account the atomic nature of the material. If the  $x$ -axis is taken parallel to the concentration gradient of the minority carriers diffusing into silicon of opposite type impurity, the flux  $J$  of the minority component along the gradient will be given by the equation

$$J = -D\left(\frac{\partial C}{\partial x}\right)_t \quad (1)$$

where  $D$  is called the diffusion constant and  $C$  is the concentration. This equation defines Fick's first law and fits the empirical behavior that the flux goes to zero as the specimen becomes homogeneous. If, however, the concentration gradient at a point is

changing with time a new equation

$$\frac{\partial C}{\partial t} = \frac{\partial}{\partial x} \left( D \frac{\partial C}{\partial x} \right) \quad (2)$$

is obtained from equation (1) by using conservation of mass. Equation (2) is called Fick's second law of diffusion. If  $D$  is not a function of position, equation (2) becomes

$$\frac{\partial C}{\partial t} = D \frac{\partial^2 C}{\partial x^2} \quad (3)$$

The diffusion constant  $D$  increases very rapidly with absolute temperature  $T$  as

$$D = D_0 e^{-\Delta H/RT}$$

where  $\Delta H$  is the activation energy.  $\Delta H$  and  $D_0$  are independent of temperature.

### Boundary Value Problems in Diffusion

The solution of equation (3) takes two forms depending on the initial boundary conditions. When the diffusion distance is short relative to the dimensions of the initial inhomogeneity,  $C(x, t)$  can be expressed in terms of error functions. However if complete homogenization is approached  $C(x, t)$  can be represented by the first few terms of an infinite trigonometric series.

Backenstoss (1) described a method for evaluation of surface

concentration of diffused layers in silicon. If the impurity distribution of a diffused layer is known, any two of the following parameters are required to describe the layer completely; the diffusion coefficient-time product, total number of diffused atoms, surface concentration, and concentration at junction depth. The surface concentration and the junction depth are the most important. The latter can be quite easily measured. Backenstoss showed how to calculate the surface concentration from the junction depth and sheet resistivity measurements under different initial boundary conditions.

For the one dimensional 'step-function' solution, we assume there is an infinite source of the diffusing impurity at the place  $x = 0$  and that it maintains a concentration in silicon of  $C = C_0$  at  $x = 0$  for all 't'. The solution of the diffusion equation then is

$$C(x) = C_0 \left[ 1 - \operatorname{erf} \frac{x}{2\sqrt{Dt}} \right] \quad (4)$$

and is shown in Figure 1. The solution can be simplified in the case  $C(x) \ll C_0$ . Then as an approximation we can put

$$\left( 1 - \operatorname{erf} \frac{x}{2\sqrt{Dt}} \right) \approx \frac{x e^{-x^2/4Dt}}{\sqrt{\pi} \sqrt{Dt}} \quad (5)$$

which gives

$$C(x) = C_0 \frac{x e^{-x^2/4Dt}}{\sqrt{\pi} \sqrt{Dt}} \quad (6)$$

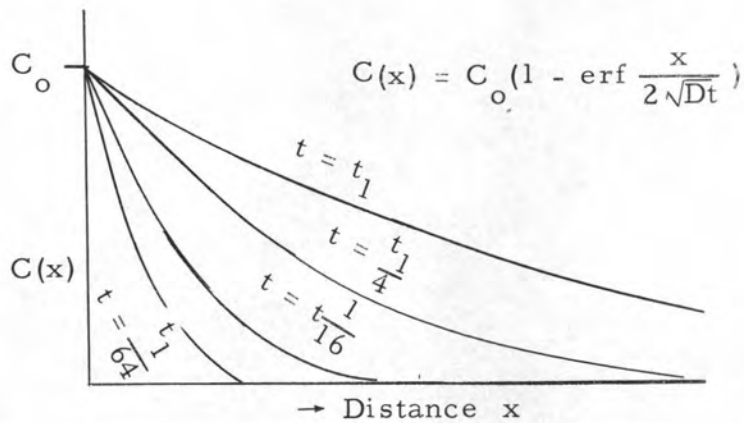


Figure 1. Step-function solution of the diffusion equation

To apply this equation to the formation of junctions we consider that if the crystal already contained an impurity of the type opposite to that diffused in, with a uniform concentration  $C'$ , then the diffusion curve will cross  $C = C'$  at the value  $x = x_0$ , the junction depth. Assuming again  $C(x) \ll C_0$  the depth of the junction will be given by

$$x_0 = 2\sqrt{Dt} \left[ \frac{C_0}{C'} - \ln \sqrt{\pi} \left( \frac{x_0}{2\sqrt{Dt}} \right) \right]^{\frac{1}{2}} \quad (7)$$

For typical value of  $C' \approx 10^{14}/\text{cc}$  which corresponds to a resistivity of about 1 ohm-cm for p-type material and  $C_0 \approx 10^{20}/\text{cm}^3$ , this expression reduces to the simple approximation

$$x_0 \approx 8\sqrt{Dt} \quad (8)$$

If the diffusion proceeds into a base already containing the diffusing impurity in the concentration  $C = C_1$  then

$$C(x) = C_1 + C_0 \left( 1 - \operatorname{erf} \frac{x}{2\sqrt{Dt}} \right) \quad (9)$$

If the total impurity amount is constant, rather than its concentration at the silicon surface, then a different solution applies

$$C(x) = \frac{Q}{\sqrt{\pi Dt}} e^{-x^2/4Dt} \quad (10)$$

where  $Q$  is the initial surface density of atoms (per square cm)

The penetration of p-n junction can again be determined by substituting  $x_0$  for  $x$  and  $C'$  for  $C$ :

$$x_0 = 2\sqrt{Dt} \left[ \ln \frac{Q}{C' \sqrt{\pi Dt}} \right]^{\frac{1}{2}} \quad (11)$$

For silicon, the initial impurity concentration  $C'$  can be calculated from the following relations (15, sec. 7-5).

For n-type

$$C' = \frac{1 \times 10^{15} / \rho}{0.73 + 0.27 \log_{10} \rho} \quad (12a)$$

and

For p-type

$$C' = \frac{2.25 \times 10^{14} / \rho}{0.73 + 0.25 \log_{10} \rho} \quad (12b)$$

where  $\rho$  is the resistivity of the material. The latter can easily be determined from the four-probe measurements (24).

$x_0$  the junction depth can be measured by angle lapping and

staining technique (9) and putting this value in equation (8), the value of the diffusion constant  $D$  can be calculated.

Sheet resistivity of a layer is another quantity which can be readily measured. The surface concentration of a diffused layer may then be obtained from the sheet resistivity and the junction depth, if the impurity distribution, the majority carrier mobilities and initial resistivity of silicon are known. If we assume that all the impurity atoms are ionized, the following relation holds for the average conductivity  $\bar{\sigma}$  of an impurity layer of thickness  $x_0$

$$\bar{\sigma} = \frac{1}{\rho_s x_0} = \frac{1}{x_0} q \int_0^{x_0} \mu(n)[C(x)-C'] dx \quad (13)$$

The sheet resistivity from four-probe measurements is

$$\rho_s = \frac{V}{I} \frac{\pi}{\ln 2} = 4.5324 \frac{V}{I} \quad (14)$$

$\mu_{(n)}$ , the majority carrier conductivity mobility in equation (13) depends on the ionized impurity density  $N$ . Since only a fraction of the impurity atoms are ionized, particularly in heavily doped silicon, an appropriate correction must be made (15 sec. 7-5). This fact can be taken into account more directly by introducing an effective  $\mu'$  defined by

$$\mu' = \frac{1}{q\rho_x N} = \frac{1}{q\rho_x C_x}$$

This is given by an analytic expression of the form

$$\begin{aligned} \mu'_{(n)} &= 300 (19 - \ln N) && \text{for } 10^{16} < N < 5 \times 10^{18} / \text{cm}^3 \\ \mu'_{(n)} &= 80 && \text{for } 5 \times 10^{18} < N < 10^{20} / \text{cm}^3 \end{aligned}$$

for electrons. Different expressions hold for holes.

The surface concentration  $C_o$  can then be evaluated as a function of  $1/\rho_s x_o$  from equations (13), (14) and (15).

### Diffusion Methods

To control the surface concentration it is necessary to control the number of impurity atoms which reach the silicon surface during the diffusion cycle. This can be done by vacuum sealing the diffusant during the diffusion cycle together with the wafers in a tube (closed-tube method); or by controlling the temperature and hence the vapor pressure, of the diffusant independent of the silicon temperature (open tube method); or by applying the diffusant directly to the wafers before heating. This last may be done by paint-on methods or in case of a metal diffusant like aluminum may be vacuum-deposited on the wafer before putting it in the furnace. Each diffusion technique has certain advantages. The method used depends on the device to be fabricated and the accuracy that is needed to secure good control on the device parameters.

In addition to these, there is the 'box method' (5) for solid state diffusion into silicon which uses an impurity oxide as a mixture

in powdered  $\text{SiO}_2$  as a source of diffusant within a loosely closed box. The surface concentration of the impurity on the silicon can then be varied over several orders of magnitude merely by variation of the source composition.

### Measurements of Diffusion in Silicon

Experimental determinations of the diffusion coefficient are usually based on the use of equations (6) and (10). The appropriate boundary conditions are maintained during the diffusion cycle. The diffusion coefficient is then found from the measurement of concentration as a function of distance from the junction. The junction depth is generally found by one of three ways. These are the use of a rectifying point contact probe, a thermoelectric point probe, and staining or other decoration of the crystal to delineate the junction. In each case the diffused wafer is lapped at a small angle to the diffusion interface. In the thermoelectric probe method when a heated point is moved across the junction the Seebeck coefficient should change from positive to negative. But since the mobility of holes and electrons is different, the zero of the Seebeck coefficient does not occur exactly at the junction where carrier concentrations are balanced.

Staining technique of locating junction depth gives very

accurate determination provided a suitable etch is used.

The junction depth can also be calculated with the help of rotating-rod equipment (19).

The layer concentration  $C(x)$  can be determined from resistivity measurements. Then, the junction depth, the diffusion time, the layer concentration being known,  $D$ , the diffusion constant can be calculated if  $C_0$  is also known. The necessity of knowing  $C_0$  can be avoided if two specimens of different resistivity are diffused simultaneously. They will then have the same surface concentration  $C_0$  but the junction depths will be different. The initial concentrations will then be related by

$$\frac{C_1}{C_2} = \frac{\operatorname{erf} [x_1/2(Dt)^{\frac{1}{2}}]}{\operatorname{erf} [x_2/2(Dt)^{\frac{1}{2}}]}$$

This two-specimen method is more accurate the greater the difference in their resistivities. This method was used by Fuller and Ditzenberger in their monumental work on diffusion of donor and acceptor elements in silicon. They lapped off the diffused sample at a very low rate ( $1\mu$  per 15 min.) and took four-point probe measurements about every micron. They observed low values for  $D$  where the diffusion distances were very small and suggested that some of the doping element may be lost by outward diffusion and thus alter the concentration at the p-n boundary.

E. Tannenbaum (26) made a detailed analysis of concentration profiles of phosphorus-diffused layers in p-type silicon by using radio-tracer techniques. She removed thin layers of silicon parallel to the junction by anodic oxidation in a 0.1 M boric acid, sodium tetraborate solution. The phosphorus in the anodized layer was removed by dissolving the oxide in HF. Radioactive counts were taken from the dissolved phosphorus. Her findings showed that the distribution is not an error-function complement under conditions of constant surface concentration. She found that the diffusion 'constant' for phosphorus increased with carrier concentration. The diffusion coefficient was found to be constant up to a concentration of about  $10^{20}/\text{cm}^3$  but is a strong function of concentration above that value. She also found that at high concentrations there was difference between the phosphorus concentration determined from resistivity measurements and that determined from radio-active tracer measurements.

Shun-ichi Maekawa (21) also found deviations from the complementary error function distribution given by the Backenstoss method. The increase of diffusion coefficient was much larger than could be accounted for by field-accelerated diffusion. He attributed the anomalies of diffusion coefficient to the existence of a fast diffusion mechanism. The surface concentration calculated

from the Backenstoss method is that of electrically active impurity, while the phosphorus concentrations obtained from radio-tracer measurements would be total ones containing electrically active and inactive phosphorus. The fast diffusion was ascribed to interstitial migration of unionized phosphorus. The fast diffusion would then be unaffected by the conductivity type and doping level of the bulk material.

Iles and Leibenhaut (16) used an etch-sectioning method combined with sheet-resistance measurements to analyze thin layers of boron and phosphorus-diffused silicon. They confirmed the above deviation from the complementary-error-function distribution. They conjectured that though out-diffusion and segregation effects are possibilities, the effect may be caused by a decrease in ionization of the fraction of impurities towards the surface because of precipitation effects or from excessive lattice strain.

Goetzberger and Shockley (10) found experimental evidence for very rapid diffusion of boron and phosphorus under strongly oxidizing conditions within a few microns of a silicon surface.

Subashiev et al (25) showed that for layers of phosphorus diffused in silicon as deep as  $35\ \mu$  normal behavior was not obeyed. To explain their results they also suggested a faster diffusion rate near the surface. Boltaks and Mateeva (2) ascribed this departure

from the normal distribution to evaporation of phosphorus during diffusion. Zaitseva and Gliberman (29) studied boron-diffused layers 10-15  $\mu$  thick with incremental etching and weighing, and measurement of the conductivity and Hall voltage in the sheet layer. They found the boron concentration essentially constant for approximately half the junction depth; this constant value was about one-tenth of that calculated from an erfc distribution, matched to the boron distribution near the junction.

Thus the hypothesis of constancy of the diffusion coefficient between the sample surface and the p-n junction has been proved to be incorrect. The mechanism of reduction of impurity oxide and of oxidation of the silicon have a strong influence on the concentration of the impurity in the silicon, but are insufficiently understood.

#### Diffusion Into Silicon Through an Oxide Layer

Frosch and Derick (7) were the first to show the feasibility of an oxide layer in protecting the silicon surface. They also showed the selective masking effects of the layer. They used an open tube diffusion method using two controlled temperature zones. A rising temperature gradient between the impurity zone and the silicon wafer heating zone avoids the redeposition of the impurity vapor before reaching the silicon sample.

D'Asaro (5) in his study of diffusion and masking carried out the diffusion in a closed box. The impurity oxide mixed with  $\text{SiO}_2$  was introduced in the box along with the silicon wafer. Most effective masking was found to result when the rate at which the impurity penetrates the  $\text{SiO}_2$  layer, is minimized. His method provides a flexible means of producing masked diffusions of boron and phosphorus in silicon and could well be adapted to other impurity oxides. He however, conceded that the mechanism of reduction of impurity oxide and of oxidation of silicon will have a strong influence on the concentration of the impurity in the silicon. The process of diffusion of impurity oxide through the silicon oxide also needed more study.

Sah, Sello and Tremere's work on diffusion of phosphorus in silicon oxide film was a step in this direction. They performed a series of experiments varying the various parameters involved to control the complete or partial masking. These parameters are: oxide thickness, diffusion temperature, diffusion time, impurity vapor pressure and impurity concentration (p-type) originally present in the silicon. They used a two-zone diffusion furnace; and p-type silicon underneath the oxide layer was used as a phosphorus detector with a hot probe. The experimental results of mask failure were analyzed by using a diffusion model. Their data indicated a

parabolic law for the growth of a phosphorus silicate compound (or glass) in silicon dioxide layer. These films were characterized by a rather homogeneous concentration and a very sharp and advancing boundary. They hypothesized that the diffusing species is probably an oxide of phosphorus diffusing in a phosphorus silicate glassy layer of an unknown composition ( $P_x Si_y O_z$ ). The rate of increase of the phosphorus silicate glass was assumed to be proportional to the net rate of the number of diffusing atoms crossing the interface. As the oxide of the phosphorus reached the glass silicon interface, phosphorus atoms enter the silicon and diffuse away. They made no attempt to describe the structural details of the glass silicon interface but ascribed a small 'segregation coefficient' to phosphorus between the glass and silicon.

Horiuchi and Yamaguchi (13) studied the diffusion of boron in silicon through the oxide layer. The results they obtained were found to be consistent with the two-boundary diffusion models formulated by Sah et al. As for phosphorus, the migration of boron through silicon dioxide was found to be a diffusion controlled reaction. The apparent diffusion constant of boron in the oxide,  $D_1$ , obtained from their experimental results was smaller than in silicon bulk  $D_2$  by a factor of nearly  $10^4$ . When the concentration of diffusant in the oxide became higher than that corresponding to the surface

concentration in silicon of  $\sim 10^{19} \text{ cm}^{-3}$  they observed a distinct increase of the diffusion in the oxide. Based on their experimental evidence they showed that the increase could be attributed to the change in the composition of the oxide.

## DIFFUSION OF ANTIMONY THROUGH A SILICON DIOXIDE LAYER

The selective masking effect of a thermally grown layer of silicon dioxide has been widely utilized as a technique for controlling the geometry and impurity concentration in the fabrication of semi-conductor devices. When a small piece of oxidized silicon is placed in a heated furnace and an impurity oxide vapor allowed to pass over it, the silicon dioxide layer acts as an absorbent for the gaseous impurity. Under equilibrium conditions the surface of the silicon dioxide layer will achieve the same composition as the source material. Then the impurity oxide at the surface of the silicon layer will act as a source for diffusion into silicon dioxide. Somewhere between the silicon dioxide - gas interface and the silicon dioxide - silicon boundary the impurity oxide will be chemically reduced. Part of this impurity-- Group III or V element -- will diffuse into the silicon. The mechanism of the reduction of impurity oxide in the silicon dioxide and its distribution therein has a strong influence on the concentration of the impurity in silicon. In spite of its wide technical application in device design the physics of the effect is hardly understood. Very little work has been done in this field. Sah et al (22), studying diffusion of phosphorus and, Horiuchi and Yamaguchi (13) in their work on boron diffusion through oxide

layer, interpreted their results in terms of a two boundary diffusion model. Both the studies showed the diffusion constant of the impurity in the oxide layer to be smaller than that in the silicon bulk. But they have not discussed the distribution of the impurity element in the oxide layer.

Antimony is one of the donor elements used for diffusion in p-type silicon. Its rate of diffusion has been found (9) to be slower than that of phosphorus or of boron. Much less work has been done on diffusion of antimony than on that of phosphorus or boron. The present endeavor is concerned with finding the distribution of antimony in the oxide layer. The different steps involved in the experimental technique are:

- 1) Selection and preparation of silicon wafers;
- 2) growing oxide layers thermally and measurement of their thickness;
- 3) diffusion process;
- 4) layer sectioning; and finally
- 5) the detection of the impurity element.

### Sample Preparation

Since antimony is a donor impurity, p-type silicon underneath the oxide layer was used as impurity detector. For the final

experiment silicon slices .92 mm thick were cut parallel to a (111) surface, from single crystal p-type ingot. They were lapped on 600 grit carbide paper on a Beuhler polisher and then polished to a smooth surface with jeweller's rouge on microcloth. The samples were then etched to a mirror finish in an etch containing five parts of concentrated nitric acid ( $\text{HNO}_3$ ) to one part of concentrated hydrofluoric acid (HF). This resulted in a final sample thickness of about .4 to .5 mm. Reproducible surfaces of excellent finish were obtained by manually shaking the etchant and keeping its temperature constant. The latter condition was obtained by holding the beaker containing the etchant in running tap water during the etching operation.

#### Growing Oxide Layers and Measurement of Their Thickness

The polished samples were washed in distilled water, in alcohol and then again in distilled water to remove any grease. Oxidation was carried out at two temperatures: 1150°C and 1200°C in an open boat in a fused quartz tube with wet oxygen flowing at a rate of 1.5 liters/min. The oxygen was bubbled through distilled water held at room temperature. The thickness of the layer could then be controlled by varying the oxidation time.

Exact measurement of the thickness of the oxide layers was

a problem. Sah et al (22) measured oxide thicknesses with a Beckman DK-2 Spectrophotometer. E. Tannenbaum (26) estimated thicknesses with comparison to color references. In the latter, color arises because of interference occurring between the light beams reflected from the upper and lower surfaces of the oxide film. Reflections of specific wavelength interfere destructively and the remaining wavelengths combine to give a characteristic color.

The thickness of the grown oxide layer could be determined quite accurately by weighing the samples in a microbalance before and after the oxide-growing process (29).

The method employed in the present experiment was to create a sloping step by removing oxide layer from a portion of the sample (3). Then interference occurs, for a parallel beam of monochromatic light, between the upper surface and lower surface of the oxide wedge. The origin of this fringe system is shown in Figure 2. The film thickness is given by

$$d = n \frac{\lambda}{2\mu} . \quad (16)$$

where  $n$  is the number of fringes in the wedge area and  $\mu$  is the refractive index for silicon dioxide,  $\lambda$  being wavelength of monochromatic light. The number of fringes  $n$  is counted from the silicon base towards the oxide film, the silicon base being considered as the center of a bright fringe.

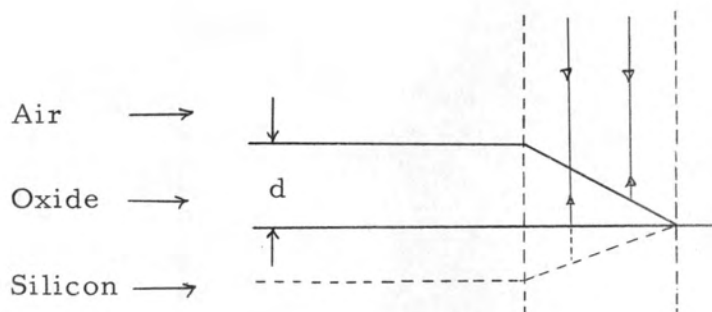


Figure 2. Origin of wedge fringes

A portion of a fringes is estimated by interpolation.

For forming a shallow wedge-shaped step in the oxide film on silicon, a piece of scotch tape was laid across the wafer and a solution of Apiezon W wax in toluene was applied with a brush to the untaped portion of silicon dioxide surface (Figure 3a)

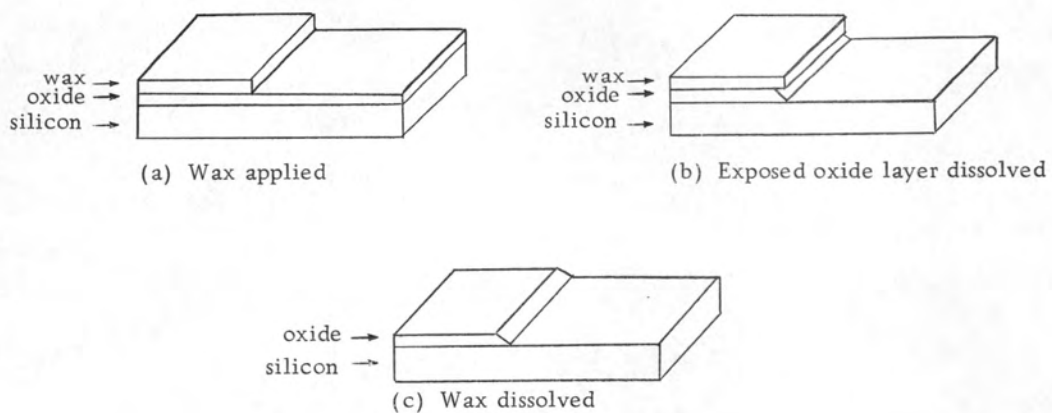


Figure 3. Oxide film step formation

The toluene rapidly evaporates, leaving a hard wax surface layer. The scotch tape was carefully removed and it left a straight edge in the wax film. The specimen was then immersed in 48 percent hydrofluoric acid for 60 seconds to dissolve the uncoated portion of the oxide film (Figure 3b). The specimen was then thoroughly rinsed in water and the wax removed by dissolving in trichloroethylene (Figure 3c). Undercutting of the wax layer by the hydrofluoric acid produces a relatively uniform wedge-shaped oxide film step. Booker and Benjamin (3) claim the angle of the wedge formed in this way to be approximately  $1^\circ$  with respect to the horizontal but present measurements showed it to be about 10 to 15 degrees.

Interference fringes were observed with a Bausch and Lomb Metallographic microscope using a magnification of 500. The monochromatic light source used was Nems-Clarke 'Merc-arc' with a filter for  $4360^\circ\text{A}$ . Photographs of the fringes were also taken. From the number of fringes the thickness of the oxide layer was calculated using equation (16). The graph (Figure 4) shows the variation of oxide layer thickness with time at the two temperatures.

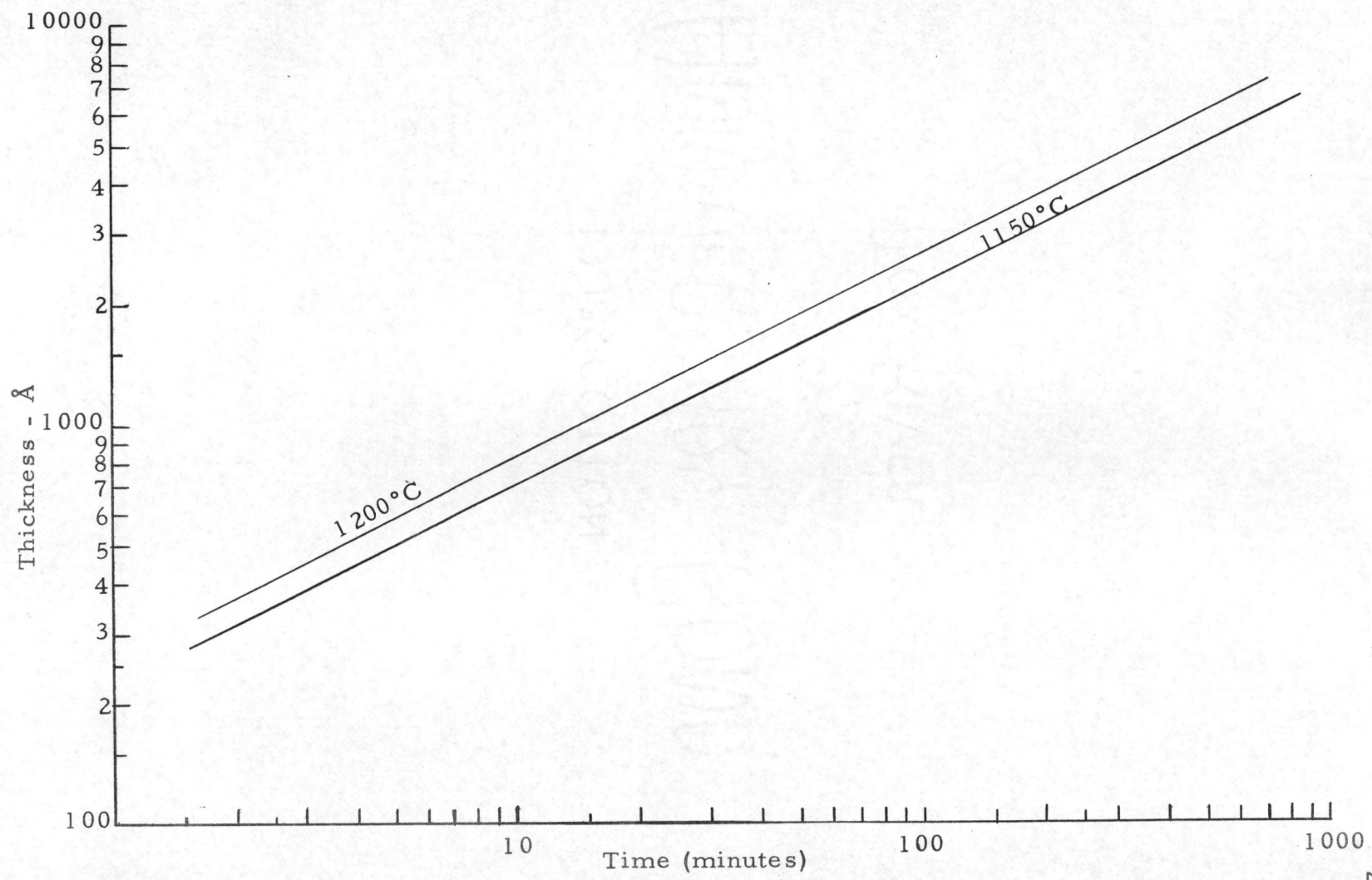


Figure 4. Silicon dioxide film thickness

### Layer Sectioning

To detect quantitatively the distribution of antimony in the silicon dioxide layer, radio-active isotope  $\text{Sb}^{122}$  was used. The half-life for this isotope is 67 hours. The problem then was to find a method for shaving off parallel sections of the oxide layer so that the activity, and hence the number of antimony atoms in a particular layer could be easily found. The prime requirement for any sectioning method is that the removal should be planar and controllable. By trial and error it was found that hydrofluoric acid of 12 percent concentration could be used to give reproducible results. Oxide layers were grown simultaneously on eight or nine silicon wafers. Sample #1 was kept as reference; sample #2 was etched in 10 mls of 12 percent HF for, say, 30 seconds; sample #3 was etched consecutively in two beakers, each containing 10 mls of 12 percent HF, for 30 secs in each; and so on for all the samples. The  $n$ th sample was thus etched consecutively in  $(n-1)$  beakers, each containing 10 mls of 12 percent HF and for a known time in each. Wedges were formed in each of these samples and their thicknesses measured by the method discussed in the last section. The plot of thickness vs etching time was found to be a straight line as shown in Figure 5. The interference fringe photographs for

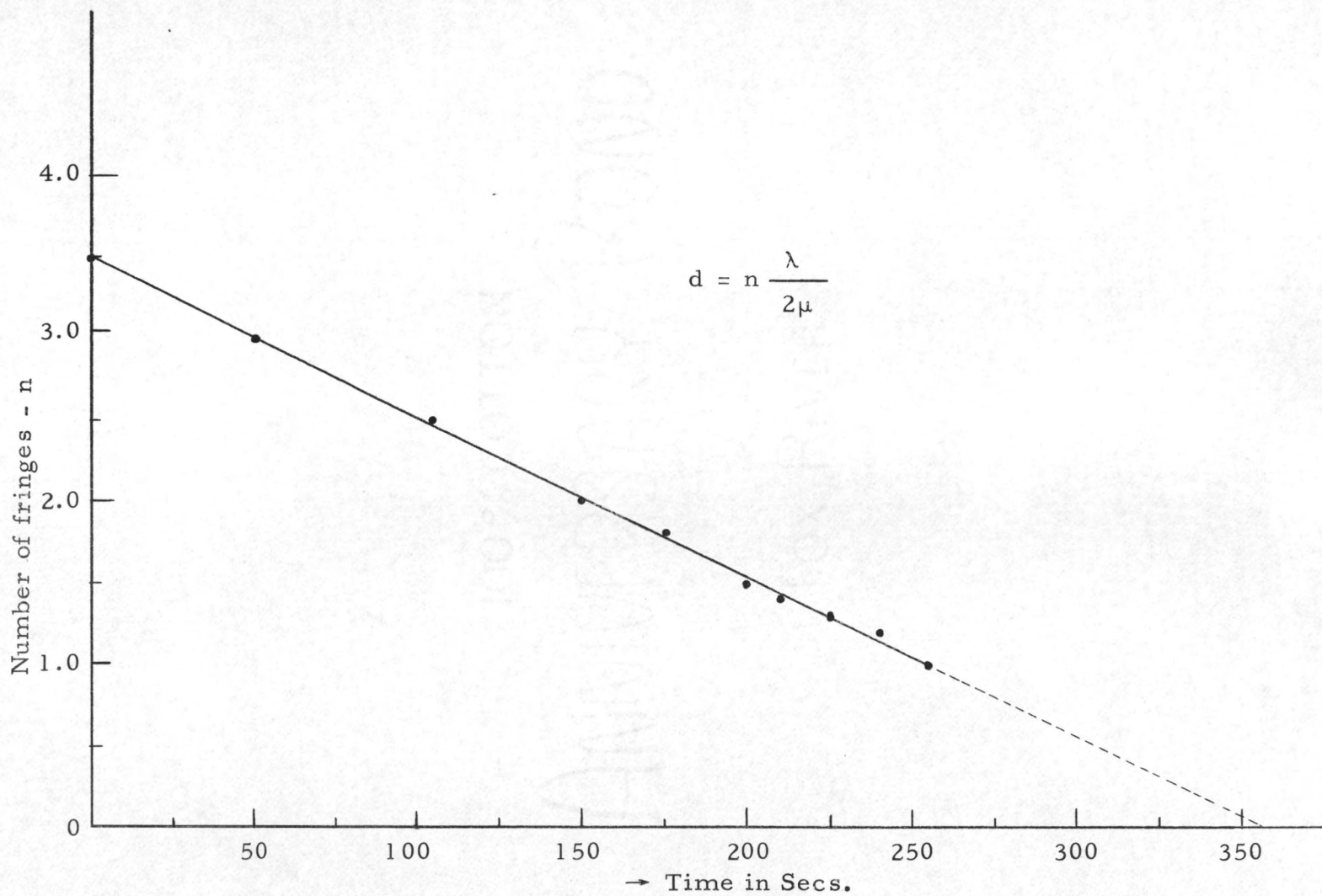


Figure 5. Etching rate  
Oxide layer thickness vs. etching time

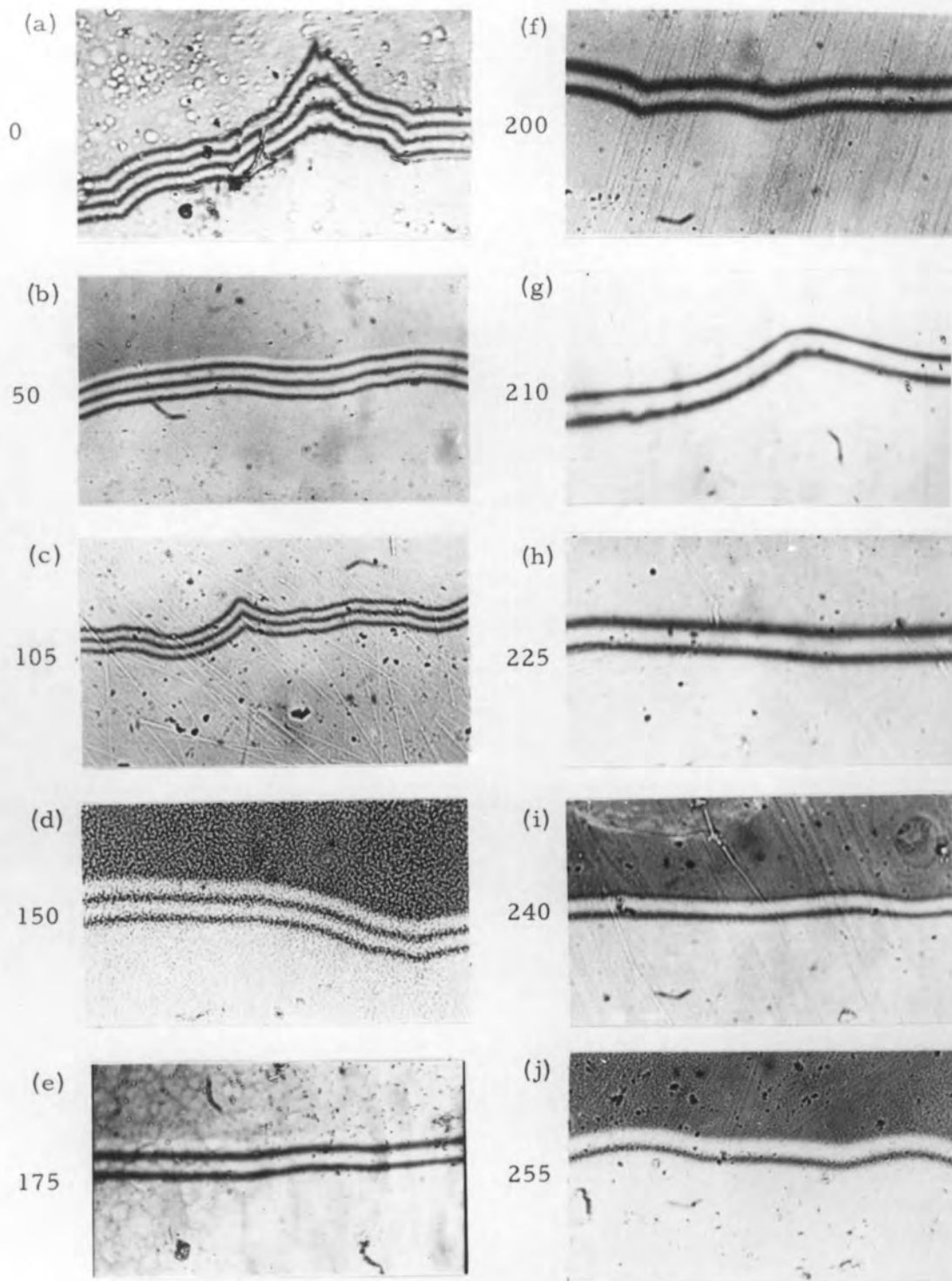
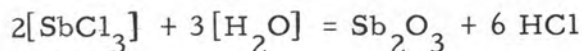


PLATE I - Typical interference fringe photographs used to determine etching rates. Numbers indicate etching times in seconds.

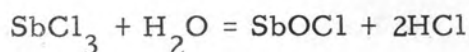
the different oxide thicknesses left after these etchings are shown in Plate I. The process was repeated with another set of samples. The results confirmed the previous observations.

### Diffusion Process

Radio-active antimony which was to be used as a tracer is available as a saturated solution of  $\text{SbCl}_3$  in  $\text{HCl}$ . Antimony trichloride could be recovered from this solution simply by evaporation of  $\text{HCl}$ . But since the melting point ( $73.4^\circ\text{C}$ ) and evaporation point ( $223^\circ\text{C}$ ) of  $\text{SbCl}_3$  are very low compared to the temperature (about  $1200^\circ\text{C}$ ) to which silicon wafers are heated in the diffusion process, antimony trichloride could not be used as such to provide the impurity vapor. A method had to be found to get some oxide of antimony from the radio-active solution. For preliminary experiments about 200 mgms of inactive antimony trichloride was dissolved in  $\text{HCl}$  and a saturated solution was obtained. Then distilled water was added to this solution for the chemical reaction



The precipitate was filtered and  $\text{Sb}_2\text{O}_3$  was obtained. The possibility of  $\text{SbOCl}$  also being obtained from the chemical reaction



was considered but infrared spectroscopic studies with a Beckman

IR-7 Spectrophotometer ruled out this possibility. The spectrum obtained showed the absence of chlorine in the residual salt. For diffusion then about 50 mgms of this oxide was put in a ceramic boat along with the silicon wafers and the boat was enclosed in a quartz tube ( $1\frac{1}{4}$ " diameter and 5" long) having a rather loose cap. The quartz tube was placed in the furnace (Figure 6) and about 500 cc/min of dry nitrogen was passed over it during the diffusion process. Diffusion was carried out for a duration depending on the thickness of the oxide layer. The time required was determined by etching off the oxide layer and using the original p-type silicon as n-type detector to see that antimony had diffused through the oxide layer and reached the silicon surface.

#### Detection of Impurity Distribution

$\text{Sb}^{122}$  is a  $\gamma$ -emitter and its presence can be detected by any of the methods used in  $\gamma$ -ray spectrometry. In this experiment, after diffusion, the oxide layer was etched off in different sections in 12 percent HF, as outlined earlier, and the activity was determined by 'well-counting' of the washings containing the etched off glass layer, by a scintillation detector. A Packard 410-A Gamma Spectrometer was used for this purpose.

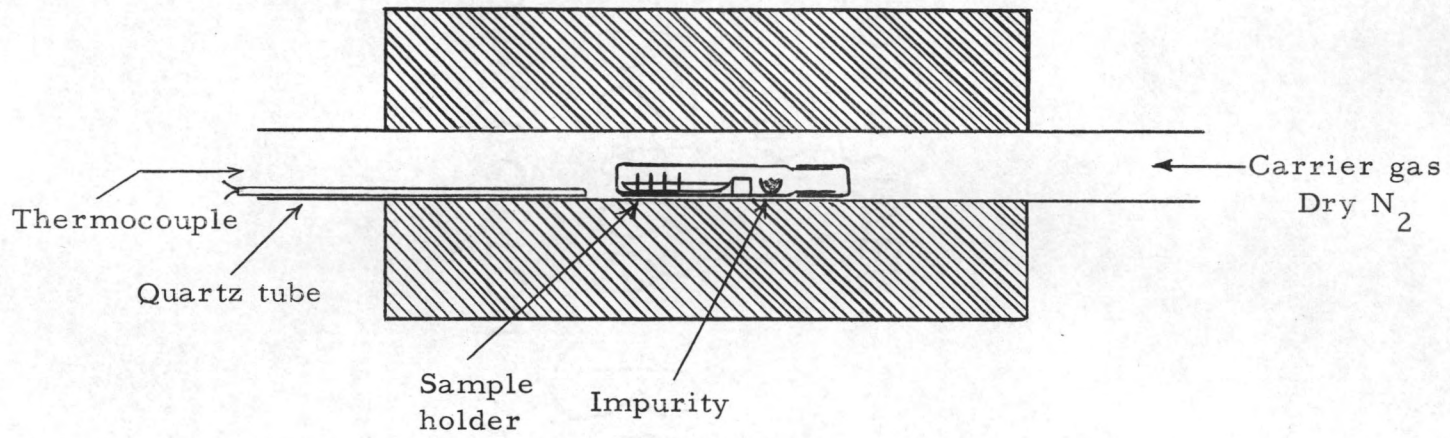


Figure 6. Diffusion Furnace

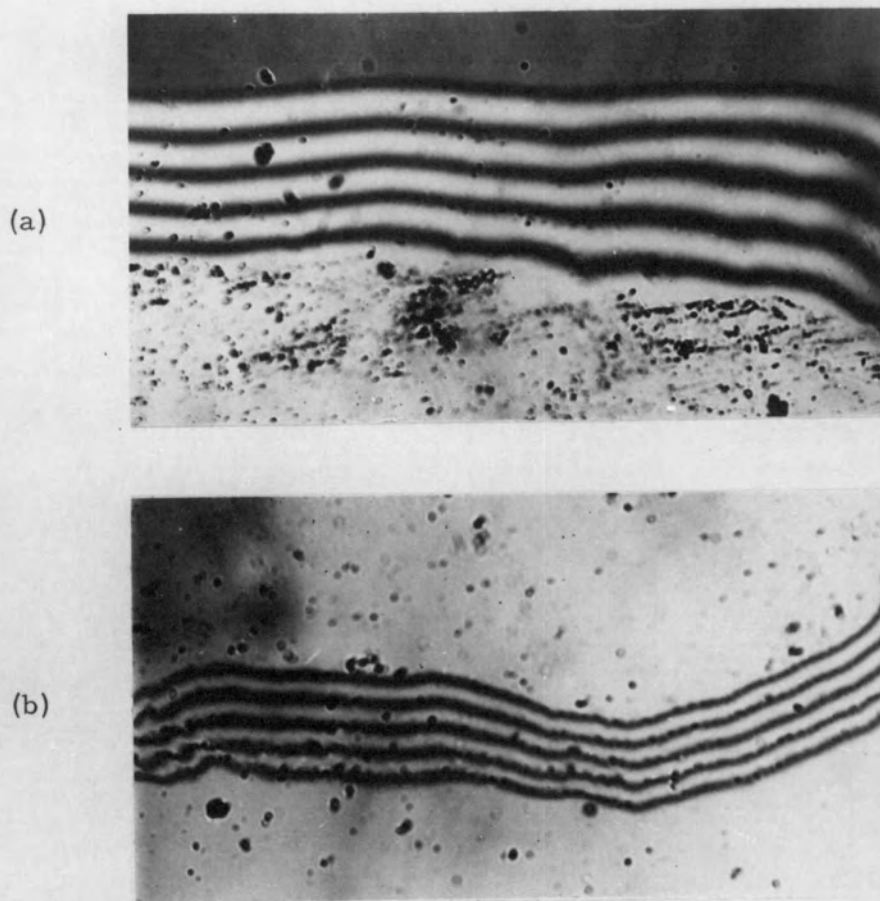


PLATE II - Interference fringe photographs of two samples used to determine final oxide layer thickness.

### Final Experiment

The experimental techniques outlined in the last four sections were perfected in preliminary experiments. For the final experiment 12 single crystal wafers of silicon were cut from the ingot, lapped, polished and etched to mirror finish. Oxide layers of thickness  $6540\text{ \AA}$  were thermally grown on them by passing wet oxygen across the wafers at  $1200^\circ\text{C}$ . On two of these samples sloping wedges were formed and the thickness measured by photographing interference fringes with the help of the metallographic microscope (see plate II). From two of the other prepared samples it was found that 14 steps of dips in 12 percent HF for 30 secs each were required to etch off the oxide thickness completely. Thus in each step, a section of oxide layer of thickness about  $6540/14 = 467\text{ \AA}$  was etched off.

About 10 milli-curies of the radio-active solution containing  $\text{SbCl}_3$  dissolved in HCl was obtained. A concentrated solution containing 200 mgms of inactive  $\text{SbCl}_3$  in HCl was mixed with the radio-active material. The radio-active  $\text{SbCl}_3$  solution had to be diluted with the inactive  $\text{SbCl}_3$  solution since using all radio-active antimony oxide in the diffusion process would be both expensive and hazardous.  $\text{Sb}_2\text{O}_3$  was obtained from this mixture by precipitation

with distilled water and filtration. This was dried under an infra-red lamp and about 50 mgms of this oxide was used in the diffusion process. Four of the twelve samples were diffused in the quartz tube for 10 hours at 1200°C. After cooling, each of these four samples was etched in 14 steps with 12 percent HF. Each of the washings was put in a numbered plastic test tube. When all the washings for the four samples were ready they were placed in the Packard Gamma Spectrometer. After each set of 14 test tubes containing washings from each silicon sample, a similar test tube containing plain distilled water was introduced in the counting 'wells'. This helped in determining the background counting rate of the gamma spectrometer without interrupting its automatic operation. The windows of the spectrometer were adjusted for maximum counting for the test specimen and the counting started. Each specimen test tube was counted for ten minutes automatically and then the next test tube in sequence was brought in. The total time for one complete run of counting the washings for the four samples plus the dummy water tubes took 10 hours and 37 minutes. The second run started automatically, repeating 10 minute counts for each specimen, starting again from number one. Five such runs were counted. As the counting continued, counts for each specimen were printed on a paper tape. The data obtained was tabulated (see Appendix). The average of the background counts was

subtracted from all the values to get the true counts due to each washing. From the counts in second and consecutive runs, the number of parent radio-active atoms of antimony (proportional to the counts in the first run) were calculated by using the formula

$$N_0 = N e^{+0.693 t/T}$$

where

$N_0$  = counts in first run

$N$  = counts in any run

$t$  = time elapsed between the first and that particular run

$T$  = half life of  $Sb^{122}$  = 67 hours

All the values of  $N_0$  obtained in this way for a particular sample were averaged and their average deviation found.

## EXPERIMENTAL RESULTS AND DISCUSSION

For each of the four samples a graph between the average counts for the section versus depth of the oxide layer section was plotted (Figure 7, p. 41). All the four samples show almost identical patterns. Since the samples were placed cross-wise in the boat, the location of the sample in the boat seems to affect the impurity concentration in it. The point corresponding to the fourth section in each sample shows a strangely anomalous behavior. Its value in each case is much higher than what would be expected from the trend of the curve in this region. This high activity by one particular section for each sample was most probably caused by contamination of the particular beaker used for etching the fourth section for each sample.

Up to the sixth or seventh section (except for point four) each sample shows a smooth curve. After this region, however, each curve shows a tendency to flatten out though the points show slight rise and fall. The fact that in this region the gamma-ray spectrometer was working near the lower limit of its sensitivity, and most likely would have some drift, may be expected to account for this deviation in counts corresponding to a flat curve. But a look at the values of the estimated average deviations (see Appendix) is sufficient

to confirm that the drift in the instrument, even if it did exist, gave results well within the experimental limits of accuracy. This average deviation is comparatively very small for the upper region. Another possibility for this variation can be the variation in etching rates for the various sections. Strictly speaking, the removal of the successive layers of the silicon dioxide by means of a manual operation in an etch cannot pretend to have an absolute accuracy. It is therefore reasonable to accept the fact that there is definitely a tendency for flattening out in this region of the curve.

From a preliminary experiment it was determined that with a diffusion time of ten hours and for the same oxide layer thickness as in the samples, the diffusant just penetrated to the  $\text{SiO}_2\text{-Si}_i$  interface. So if it be assumed that the thickness of the oxide layer represents the junction depth, then from equation (8) the approximate value for diffusion constant of antimony in the silicon dioxide layer comes out to be  $1.84 \times 10^{-15} \text{ cm}^2/\text{sec}$ . This is of the order as expected since the value for diffusion constant for antimony in silicon at  $1200^\circ\text{C}$  is  $2.5 \times 10^{-13} \text{ cm}^2/\text{sec}$ . (9) and checks with the work of Sah et al (22) and, Horiuchi and Yamaguchi (13) who found the value for diffusion constant for phosphorus and boron, respectively to be smaller in silicon dioxide than in silicon.

In the present investigation the experimental conditions were such that the solution to the differential equation was subject to the initial boundary condition

$$\begin{array}{lll} C = 0 & x > 0 & t = 0 \\ \text{and} & & \\ C = C_0 & x = 0 & t > 0 \end{array}$$

where  $C_0$  is constant. If the diffusion constant  $D$  is assumed to be really constant, the solution of the diffusion equation will be

$$C = C_0 \operatorname{erfc} \frac{x}{\sqrt{4Dt}}$$

It can be justifiably assumed that the percentage of the radioactive antimony atoms in the total active-inactive antimony mixture atoms is the same in the oxide layer as outside on the surface.

Further from the shape of the erfc curve it is quite reasonable to assume that the concentration in the first section (467 Å below the top surface), is about the same as  $C_0$ . Then for sample #3 taking the counts for the first section as  $C_0$  and the value of the diffusion constant as calculated from equation (8) the error function complement distribution was plotted (curve I, Figure 8). This shows a much more abrupt drop than the experimental curve (curve II).

Curve III has been plotted, following the method of Zeitzava et al (29), from the two experimental points 1 and 2 of curve II.

This has a value of diffusion constant  $D = 7.40 \times 10^{-15} \text{ cm}^2/\text{sec}$ .

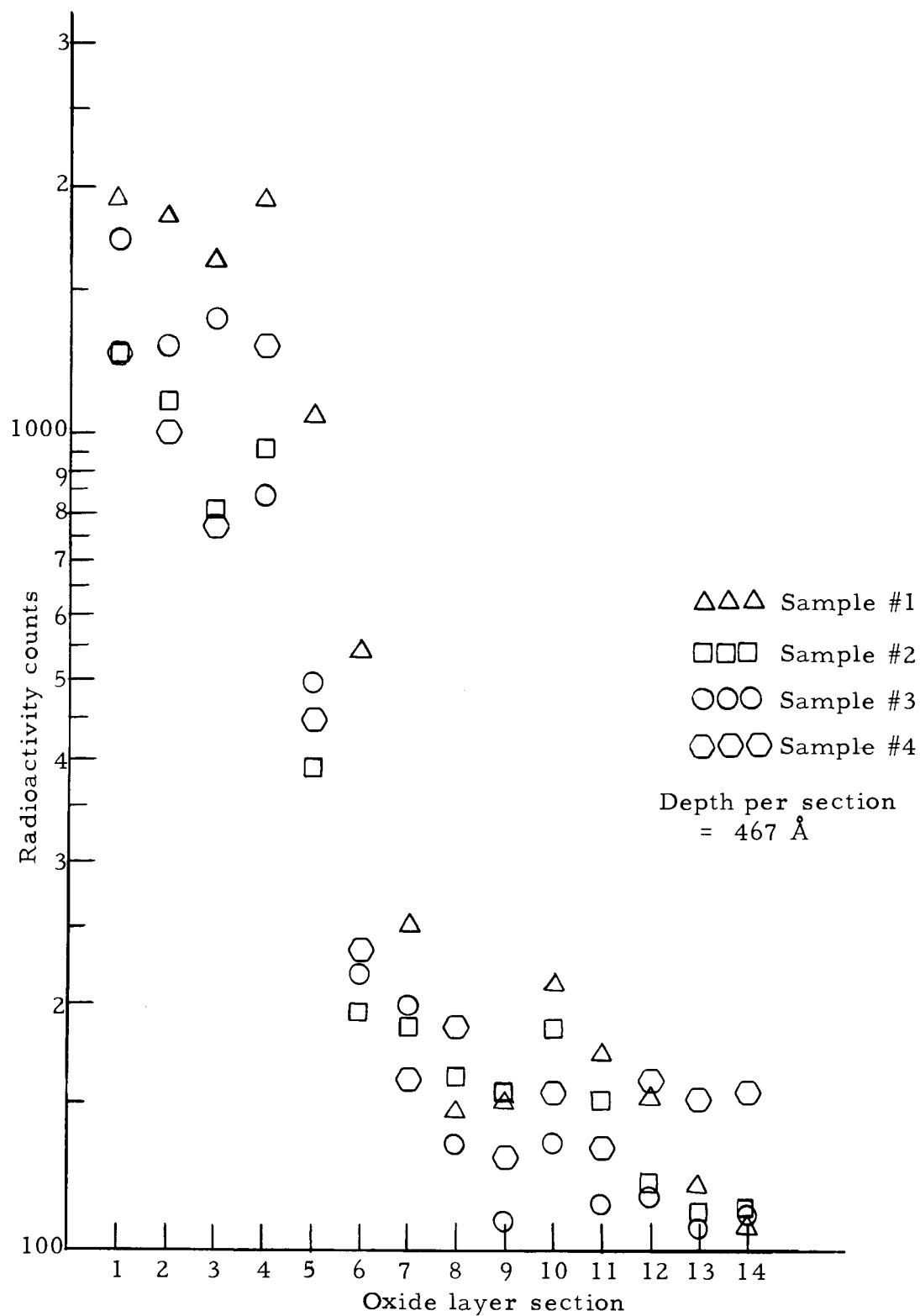


Figure 7. Radio-active counts vs. oxide layer section

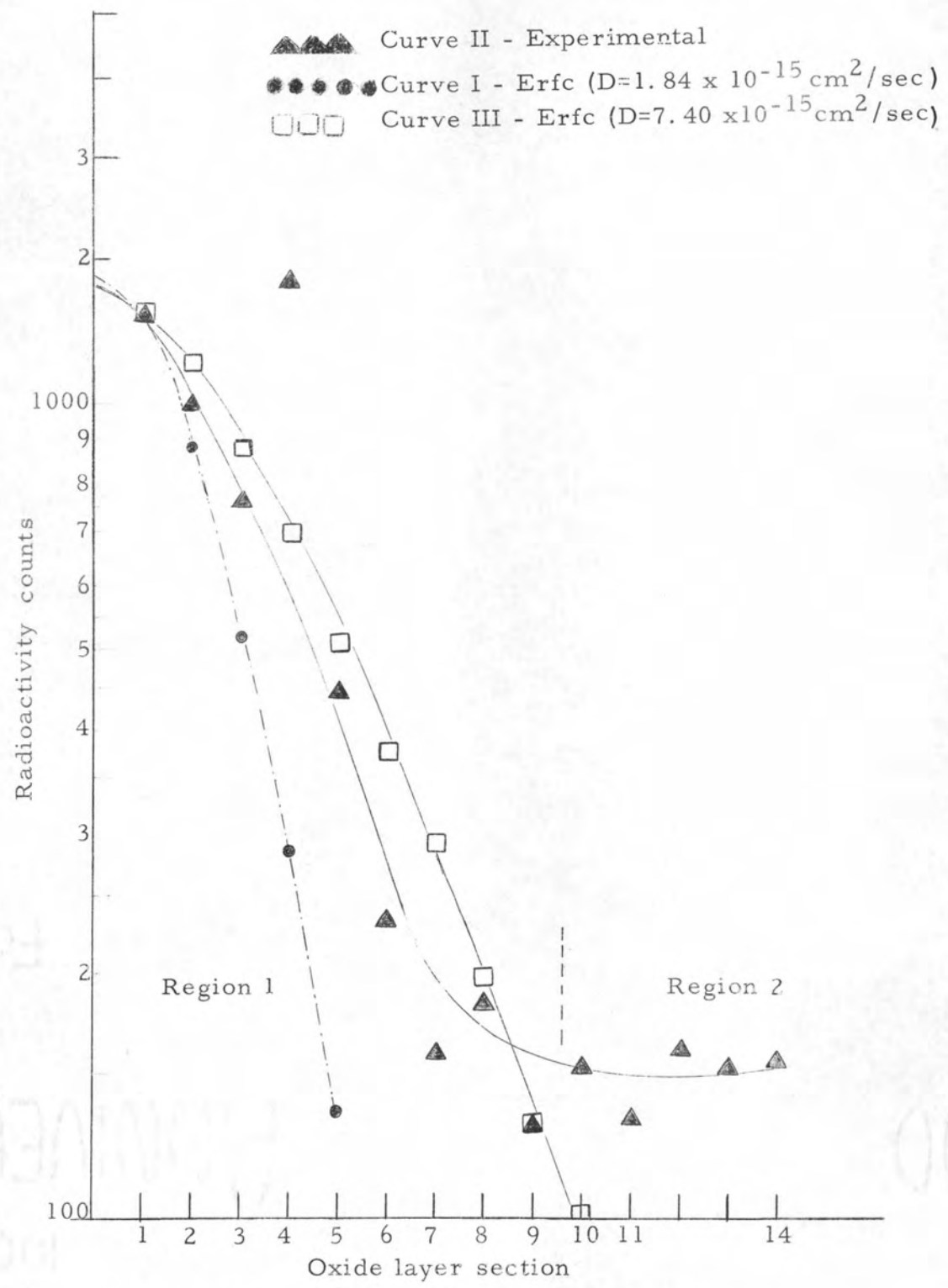


Figure 8. Comparison with erfc distribution

and follows almost the contour of the experimental curve in region I.

So from the experimental evidence it can be stated that the migration of antimony through the silicon-dioxide layer is a diffusion controlled reaction and the concentration profile of antimony diffusing in this layer can be broken up into two regions. The diffusion follows an approximate erfc distribution in the first region with a diffusion constant =  $7.40 \times 10^{-15} \text{ cm}^2/\text{sec}$ . The second region, however, shows a saturation behavior with the distribution remaining constant up to the silicon dioxide-silicon interface.

## BIBLIOGRAPHY

1. Backenstoss, G. Evaluation of surface concentration of diffused layers in silicon. *Bell System Technical Journal* 37:699-710. 1958.
2. Boltaks, B. I. and N. N. Mateeva. The problem of diffusion of phosphorus in silicon. *Soviet Physics - Solid State* 4:444-447. 1962.
3. Booker, G. R. and G. E. Benjamin. Measurement of thickness and refractive index of oxide films on silicon. *Journal of the Electrochemical Society* 109:1206-1212. 1962.
4. Crank, J. *Mathematics of diffusion*. Oxford, Clarendon Press, 1956. 247 p.
5. D'Asaro, L. A. Diffusion and oxide masking in silicon by the box method. *Solid - State Electronics* 1:32-12. 1960.
6. \_\_\_\_\_ . Slicing thin-sections of semiconductors. Gillings-Brownwill thin sectioning machine. *Electronics* 33:154-155. 1960.
7. Frosch, C. J. and L. Derick. Surface protection and selective masking during diffusion in silicon. *Journal of the Electrochemical Society* 104:547-552. 1957.
8. Fuller, C. S. and J. A. Ditzenberger. Diffusion of boron and phosphorus in silicon. *Journal of Applied Physics* 25:1439. 1954.
9. Fuller, C. S. and J. A. Ditzenberger. Diffusion of donor and acceptor elements in silicon. *Journal of Applied Physics* 27:544-553. 1956.
10. Goetzberger, Adolf and William Shockley. Anomolously high diffusion of boron and phosphorus from oxide layers on silicon at 700 to 900°C. *Bulletin of the American Physical Society* 4:455. 1959.

11. Hannay, N. B. Semiconductors. New York, Reinhold Publishing Corp., 1959. 767 p.
12. Heikes, Robert R. and Roland W. Ure, Jr. Thermoelectricity: science and engineering. New York, Interscience Publishers, 1961. 576 p.
13. Horiuchi, Shiro and Jiro Yamaguchi. Diffusion of boron through oxide layer. Japanese Journal of Applied Physics 1:314-323. 1962.
14. Hughes, H. E. and J. O. Maloney. Application of radio-active tracers to diffusional operations. Chemical Engineering Progress 48:192. Apr. 1952.
15. Hunter, Lloyd P. Handbook of semiconductor electronics. New York, McGraw Hill Book Co. Inc., 1956. 1 vol. (various pagings)
16. Iles, P. A. and B. Leibenhaut. Diffusant impurity-concentration profiles in thin layers of silicon. Solid State Electronics 5:331-339. 1962.
17. Jost, W. Diffusion in solids, liquids and gases. New York, Academic Press Inc., 1952. 558 p.
18. Kuczynski, G. C. A new method of measuring diffusion coefficient in solids with radio-active tracers. Journal of Applied Physics 19:308. 1948.
19. Looney, J. C. Department of Electrical Engineering, Oregon State University, Private communication.
20. Mackintosh, I. M. The diffusion of phosphorus in silicon. Journal of the Electrochemical Society 109:392-401. 1962.
21. Maekawa, S. Diffusion of phosphorus into silicon. Journal of the Physical Society of Japan 17:1592-1597. 1962.
22. Sah, C. T., H. Sello and D. A. Tremere. Diffusion of phosphorus in silicon oxide films. Journal of Physics and Chemistry of Solids 11:288-298. 1959.

23. Shewmon, Paul G. Diffusion in solids. New York, McGraw Hill, 1963. 202 p.
24. Smits, F. M. Measurement of sheet resistivities with the four-point probe. Bell System Technical Journal 37:711. 1958.
25. Subashiev, V. K., A. P. Landsman and A. A. Kukharskii. Distribution of phosphorus atoms during diffusion in silicon. Soviet Physics - Solid State 2:2406-2411. 1961.
26. Tannenbaum, E. Detailed analysis of thin phosphorus-diffused layers in p-type silicon. Solid State Electronics 2:123-132. 1961.
27. Tolansky, S. Multiple-beam interferometry of surfaces and films. Oxford, Clarendon Press, 1948. 187 p.
28. Tolansky, S. Surface microtopography. New York, Interscience Publishers, 1960. 296 p.
29. Zaitseva, A. K. and A. Ya. Gliberman. Study of dopant distribution in the surface layer of photoelectric solar energy converters made from n-type silicon. Soviet Physics - Solid State 3:1724-1727. 1962.

## APPENDIX

Section Number	SAMPLE # 1											SAMPLE # 2										
	Run #1	Run # 2		Run #3		Run #4		Run #5		Average	Average Deviations	Run #1	Run #2		Run #3		Run #4		Run #5		Average	Average Deviations
	N <sub>1</sub> =N <sub>o</sub>	N <sub>2</sub>	N <sub>o</sub>	N <sub>3</sub>	N <sub>o</sub>	N <sub>4</sub>	N <sub>o</sub>	N <sub>5</sub>	N <sub>o</sub>	N <sub>o</sub>		N <sub>1</sub> =N <sub>o</sub>	N <sub>2</sub>	N <sub>o</sub>	N <sub>3</sub>	N <sub>o</sub>	N <sub>4</sub>	N <sub>o</sub>	N <sub>5</sub>	N <sub>o</sub>	N <sub>o</sub>	
1	1902	1719	1920	1533	1910	1397	1940	1237	1920	1918	4.46	1130	1058	1180	1024	1270	896	1250	817	1265	1241	15.35
2	1862	1552	1735	1353	1690	1221	1700	1225	1900	1775	36.6	1122	974	1085	831	1030	749	1040	741	1149	1085	18.7
3	1629	1465	1630	1248	1552	1175	1635	1055	1640	1617	9.9	742	725	810	640	795	570	795	557	865	801	12.9
4	1975	1656	1850	1556	1940	1332	1860	1250	1935	1912	20.4	977	836	935	735	915	709	985	629	975	957	11.6
5	1009	917	1020	830	1032	746	1039	680	1050	1030	5.55	401	357	399	269	335	279	388	233	362	387	6.5
6	526	498	555	449	558	391	546	321	499	537	8.65	212	172	192	167	208	131	182	103	160	191	7.05
7	227	186	207	224	279	210	292	148	230	247	13.8	202	164	183	111	138	116	161	129	200	186	7.25
8	142	216	241	114	142	109	152	98	152	147	2.5	183	141	157	120	149	118	164	136	211	163	5.1
9	134	171	191	108	134	102	142	56	87	150	10.1	167	155	173	106	132	120	167	84	131	154	8.02
10	221	199	222	171	213	142	197	93	144	213	4.1	159	155	173	161	200	130	181	141	219	186	8.20
11	180	161	179	125	156	125	174	111	172	172	3.8	172	153	171	118	147	103	144	81	125	150	6.9
12	127	140	156	144	179	133	185	75	116	153	11.1	105	112	125	94	117	96	133	77	119	120	3.30
13	140	106	118	98	122	91	126	58	90	119	5.45	126	147	164	90	112	41	57	58	90	110	12.9
14	86	93	103	105	131	78	108	63	98	105	5.1	120	153	171	89	111	144	200	69	107	113	2.8

APPENDIX

Section Number	SAMPLE #3											SAMPLE #4												
	Run #1		Run #2		Run #3		Run #4		Run #5		Average	Average Deviations	Run #1		Run #2		Run #3		Run #4		Run #5		Average	Average Deviations
	N <sub>1</sub> =N <sub>0</sub>	N <sub>2</sub>	N <sub>0</sub>	N <sub>3</sub>	N <sub>0</sub>	N <sub>4</sub>	N <sub>0</sub>	N <sub>5</sub>	N <sub>0</sub>	N <sub>0</sub>	N <sub>1</sub> =N <sub>0</sub>		N <sub>2</sub>	N <sub>0</sub>	N <sub>3</sub>	N <sub>0</sub>	N <sub>4</sub>	N <sub>0</sub>	N <sub>5</sub>	N <sub>0</sub>	N <sub>0</sub>	N <sub>0</sub>		
1	1736	1508	1680	1317	1640	1214	1690	1154	1790	1707	20.0	1210	1141	1270	993	1230	927	1290	796	1235	1247	11.8		
2	1264	1152	1285	1030	1280	899	1250	823	1273	1270	4.83	1063	863	965	815	1010	678	946	630	976	992	15.9		
3	1320	1210	1350	1034	1285	952	1325	788	1220	1320	8.72	778	716	800	626	780	520	725	485	751	767	10.2		
4	832	757	845	623	775	622	866	551	856	833	11.5	1323	1226	1367	1059	1320	951	1320	899	1390	1344	12.3		
5	498	441	493	400	496	359	500	322	500	497	1.07	387	407	455	377	470	346	483	263	407	440	15.5		
6	218	217	242	195	242	144	200	170	264	233	8.75	245	194	216	181	225	176	245	148	230	232	4.55		
7	203	204	227	148	184	132	184	126	195	199	5.9	182	130	145	127	158	123	171	88	136	158	6.42		
8	103	148	165	97	120	94	131	94	146	133	8.02	197	135	151	162	201	132	183	120	186	184	5.9		
9	108	106	118	79	98	73	102	69	107	107	2.31	165	126	141	88	109	74	103	78	121	128	8.12		
10	106	137	153	109	135	110	153	80	124	134	6.9	155	141	157	112	139	103	144	110	170	153	4.01		
11	119	58	65	106	132	63	88	37	57	113	9.55	166	94	105	90	112	94	130	92	142	131	8.2		
12	133	94	105	78	97	90	125	74	115	115	5.0	148	161	180	96	119	114	158	125	194	160	9.8		
13	98	68	76	101	125	69	96	84	130	105	8.02	164	130	145	100	124	132	184	90	139	151	8.12		
14	91	119	133	84	104	57	79	99	153	112	11.1	156	111	124	107	133	129	180	117	181	155	9.4		